Cellular communication network 2 (connective tissue growth factor) aggravates acute DNA damage and subsequent DNA damage response-senescence-fibrosis following kidney ischemia reperfusion injury

Check for updates

OPEN

Floris A. Valentijn[1], Sebastiaan N. Knoppert[1], Laura Marquez-Exposito[2], Raúl R. Rodrigues-Diez[2], Georgios Pissas[3], Jiaqi Tang[4], Lucia Tejedor-Santamaria[2], Roel Broekhuizen[1], Rohan Samarakoon[4], Theodoros Eleftheriadis[3], Roel Goldschmeding[1], Tri Q. Nguyen[1], Marta Ruiz-Ortega[2] and Lucas L. Falke[1]

[1]Department of Pathology, University Medical Center Utrecht, Utrecht, the Netherlands; [2]Molecular and Cellular Biology in Renal and Vascular Pathology, Fundación Instituto de Investigación Sanitaria -Fundación Jiménez Díaz, Universidad Autónoma Madrid, Madrid, Spain; [3]Department of Nephrology, Faculty of Medicine, University of Thessaly, Larissa, Greece; and [4]Center for Cell Biology and Cancer Research, Albany Medical Center, Albany, New York, USA

Chronic allograft dysfunction with progressive fibrosis of unknown cause remains a major issue after kidney transplantation, characterized by ischemia-reperfusion injury (IRI). One hypothesis to account for this is that spontaneous progressive tubulointerstitial fibrosis following IRI is driven by cellular senescence evolving from a prolonged, unresolved DNA damage response (DDR). Since cellular communication network factor 2 ((CCN2), formerly called connective tissue growth factor), an established mediator of kidney fibrosis, is also involved in senescence-associated pathways, we investigated the relation between CCN2 and cellular senescence following kidney transplantation. Tubular CCN2 overexpression was found to be associated with DDR, loss of kidney function and tubulointerstitial fibrosis in both the early and the late phase in human kidney allograft biopsies. Consistently, CCN2 deficient mice developed reduced senescence and tubulointerstitial fibrosis in the late phase; six weeks after experimental IRI. Moreover, tubular DDR markers and plasma urea were less elevated in CCN2 knockout than in wild-type mice. Finally, CCN2 administration or overexpression in epithelial cells induced upregulation of tubular senescence–associated genes including p21, while silencing of CCN2 alleviated DDR induced by anoxia-reoxygenation injury in cultured proximal tubule epithelial cells. Thus, our observations indicate that inhibition of CCN2 can mitigate IRI-induced acute kidney injury, DNA damage, and the subsequent DDR-senescence-fibrosis sequence. Hence, targeting CCN2 might help to protect the kidney from transplantation-associated post-IRI chronic kidney dysfunction.

Correspondence: *Floris A. Valentijn, Department of Pathology, H04.312, UMC Utrecht, Heidelberglaan 100, 3584 CX, Utrecht, the Netherlands. E-mail: F.A.Valentijn@umcutrecht.nl*

Received 8 October 2021; revised 17 May 2022; accepted 23 June 2022; published online 31 July 2022

Kidney International (2022) **102,** 1305–1319; https://doi.org/10.1016/j.kint.2022.06.030

KEYWORDS: cellular communication network factor 2; cellular senescence; chronic kidney disease; DNA damage response; ischemia-reperfusion injury; tubulointerstitial fibrosis

Translational Statement

Our data suggest that anti–cellular communication network factor 2 (CCN2) therapy may help to prevent chronic allograft dysfunction by limiting ischemia-reperfusion injury (IRI)–induced acute DNA damage, senescent cell accumulation, and subsequent tubulointerstitial fibrosis. Anti-CCN2 therapy could therefore improve graft function and survival outcomes in patients. Several pharmacologic inhibitors of CCN2 have proven safe and tolerable in phase 1 and/or 2 clinical trials for several indications, including senescence- and fibrosis-associated diseases. The next steps toward clinical application of anti-CCN2 therapy in patients who underwent kidney transplantation include experimental IRI studies using pharmacologic inhibitors of CCN2 and addressing the right timing of therapy.

Chronic allograft dysfunction (CAD) due to tubulointerstitial fibrosis is the leading cause of kidney allograft loss and may develop without identifiable cause, despite adequate immunosuppression. Ischemia-reperfusion injury (IRI), in which ischemia is followed by reoxygenation injury, is the main cause of acute kidney injury associated with transplantation surgery and considered a major cause of CAD. CAD is defined by progressive tubulointerstitial fibrosis, functional decline, and eventual loss of the

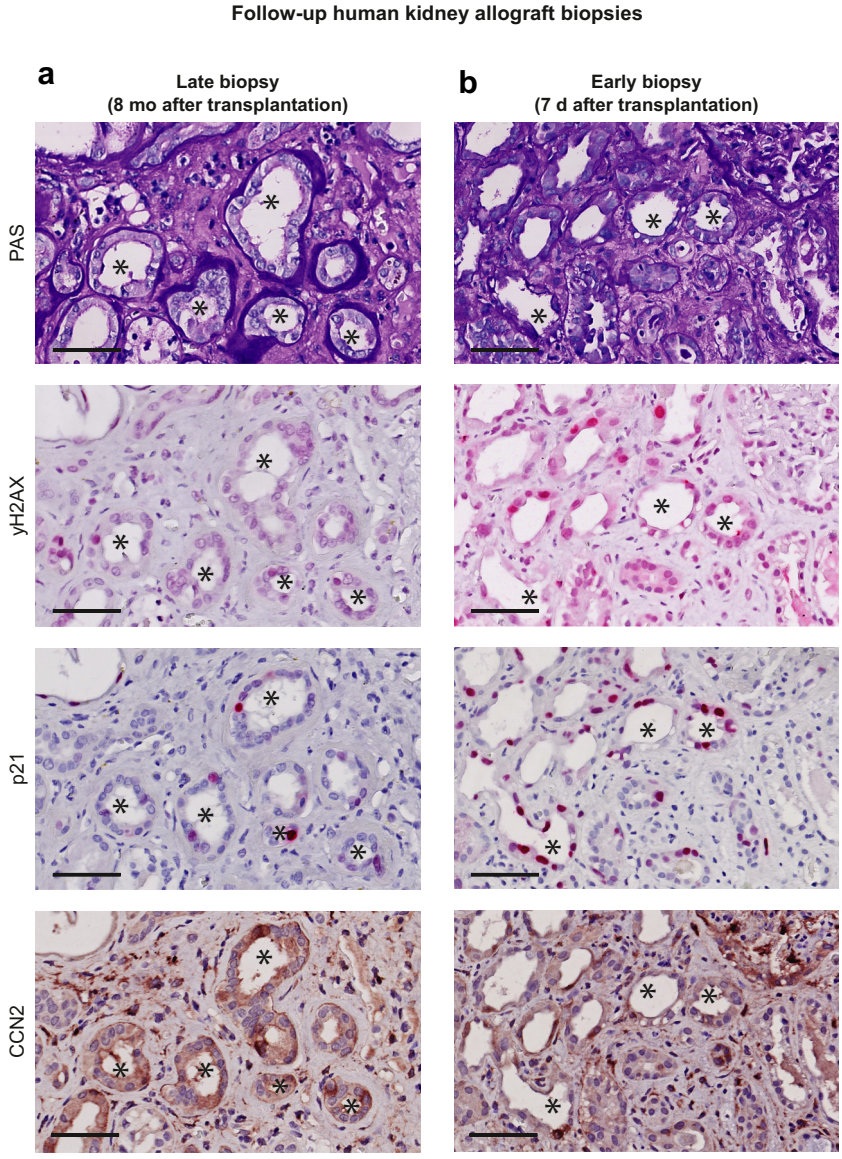

Figure 1 | Tubular expression of cellular communication network factor 2 (CCN2) colocalizes with DNA damage response in an early and late biopsy of the same kidney allograft. (**a**,**b**) Representative micrographs of renal cortex tissue derived from the same kidney allograft biopsied (**a**) 8 months and (**b**) 7 days after transplantation. Images depict consecutive sections stained with periodic acid–Schiff (PAS), gamma H2AX (γH2AX), p21CIP1 (p21), and CCN2. Asterisks indicate the same renal tubules expressing γH2AX, p21, and CCN2. Bar = 100 μm. To optimize viewing of this image, please see the online version of this article at www.kidney-international.org.

kidney graft.[1,2] Short-term allograft survival has improved substantially over the past decades, but long-term outcomes remain poor.[3,4] Given the high demand for suitable donor kidneys and their limited availability, prolonging survival of allografts is of utmost importance.

Cell cycle arrest (CCA) is a physiological process and essential for the repair of DNA damage immediately after injury.[5] Unsuccessful DNA repair either results in apoptosis or alternatively, in cellular senescence with persistence of a DNA damage response (DDR). Cellular senescence has been defined as a state of persistent, irreversible CCA that may lead to detrimental adverse tissue remodeling via dedifferentiation and by the associated phenomenon dubbed the senescence-associated secretory phenotype (SASP) characterized by the secretion of proinflammatory and profibrotic stimuli.[6–9] In the kidney, cellular senescence is associated with the development of tubulointerstitial fibrosis after transplantation surgery–induced IRI.[10–13] Interestingly, in experimental ageing, elimination of senescent cells preserved kidney function.[14,15] In unilateral IRI, treatment with the "senolytic" agents dasatinib and quercetin reduced tubulointerstitial fibrosis.[16]

Cellular communication network factor 2 (CCN2), previously known as connective tissue growth factor, is a matricellular protein involved in IRI and fibrosis. It contributes to tubulointerstitial fibrosis in CAD and has successfully been targeted to limit fibrosis.[17] CCN2 is involved in various

processes, including cell proliferation, differentiation, adhesion, and angiogenesis, and promotes inflammation and fibrosis.[17–19] CCN2 is also implicated in cellular senescence. It is not only a prominent SASP factor but can also function by itself as a cellular survival factor and as an inducer of cellular senescence *in vitro*.[20–22]

Observing colocalization of CCN2 with DDR and senescence markers in an early and late biopsy of the same human kidney allograft led us to hypothesize that CCN2 could contribute to senescent cell accumulation and tubulointerstitial fibrosis during CAD development after IRI. To elucidate this hypothesis, we investigated the relation between CCN2 and cellular senescence in the early and late phase of human kidney allograft biopsies, in a bilateral IRI model in CCN2 knockout (KO) mice, in CCN2-treated mice and cultured cells, and finally, in an anoxia-reoxygenation (AR) model in CCN2-silenced cultured cells.

METHODS

Human kidney specimens

Tissue sections were derived from routine clinical kidney allograft biopsies at the University Medical Center Utrecht. Follow-up biopsies were taken 7 days and 8 months after transplantation from a 55-year-old man, with a creatinine at biopsy of 1498 μmol/l and 779 μmol/l, respectively. Indication biopsies for delayed graft function (DGF) 6–8 days after transplantation and protocol biopsies 5–29 years after transplantation served as early and late phase specimens. All transplants were derived from nonliving donors. All patient samples were leftover body material from clinical biopsies and were collected according to the institutional ethical guidelines. Samples were anonymized, which allowed us to use this redundant tissue for research purposes, without requirement of informed patient consent.[23]

Animals

All animal procedures were performed according to the Animal Research: Reporting of *In Vivo* Experiments guidelines and with consent of the local Experimental Animal Ethics Committees.[24] Generation of tamoxifen-inducible CCN2-full KO mice is described elsewhere.[25] In brief, $CCN2^{Flox/Flox}$ mice were crossbred with ROSA26CreERT2 mice ($Gt(ROSA)26Sor^{tm(cre/ERT2)Tyj}$/J, the Jackson Laboratory), both on a C57Bl6/J background. For i.p injection, tamoxifen citrate was dissolved in corn oil (Sigma Aldrich) in a 10 mg/ml concentration. To induce recombination, 12- to 14-week-old male mice received 4 i.p. injections on alternate days over a course of 7 days with 100 μl of tamoxifen-corn oil solution. Littermates injected with vehicle corn oil using the same regimen were used as control mice (referred to as wild-type [WT] mice). Treatments were performed in a blinded fashion. After the last injection, a 14-day washout period was followed by the IRI operation.

Ischemia-reperfusion injury model

IRI was executed as previously described.[26] Renal pedicles were located through an abdominal midline incision and bilaterally clamped for 25 minutes with neurovascular clamps. Clamping and subsequent reperfusion-associated color changes were visually confirmed. IRI mice without color changes were excluded. Sham-operated mice underwent the same procedure without the pedicle clamping. Mice were anesthetized with 2% isoflurane, and body temperature was maintained at 37 °C. The operator was blinded for the treatment group. After 3 days or 6 weeks, mice were euthanized by lethal dose ketamine-xylazine-acepromazine injection, and plasma and organs were collected and stored at −80 °C.

Cell cultures

Mouse primary renal proximal tubule epithelial cells (RPTECs; C57-6015; Cell Biologics) were cultured as described previously using 100 ng/ml recombinant CCN2 (Peprotech, 120-19) and a GasPak EZ Anaerobe Container System with indicator (cat. no. 26001; BD Biosciences).[27] Etoposide (1.5 μg/ml; E1383-25MG; Sigma-Aldrich) was used as positive control for senescence. Gene silencing was performed using predesigned small, interfering RNA corresponding to CCN2 (small, interfering RNA ID MSS274358; Thermo-fisher) according to the manufacturer's protocol. In short, subconfluent cells were transfected in Opti-MEM–reduced serum medium (Invitrogen) for 24 hours with 5 ng/ml small, interfering RNA using 50 nM Lipofectamine RNAi-MAX (Invitrogen), followed by 24 hours of incubation in 20% fetal bovine serum medium and 24 hours of incubation in serum-free medium. Controls were nontransfected

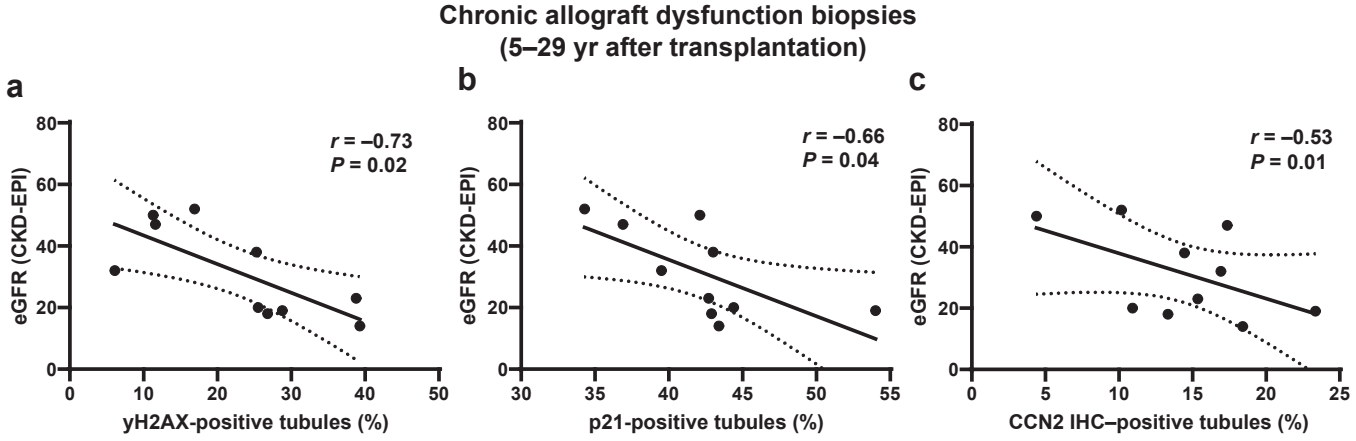

Figure 2 | Tubular expression of cellular communication network factor 2 (CCN2) and DNA damage response are associated with kidney function in chronic allograft dysfunction (CAD) biopsies. (**a–c**) Estimated glomerular filtration rate (eGFR) correlated with (**a**) cortical tubular gamma H2AX (γH2AX) and (**b**) p21CIP1 (p21) and trended to correlate with (**c**) CCN2 expression in CAD biopsies. CKD-EPI, Chronic Kidney Disease Epidemiology Collaboration; IHC, immunohistochemistry.

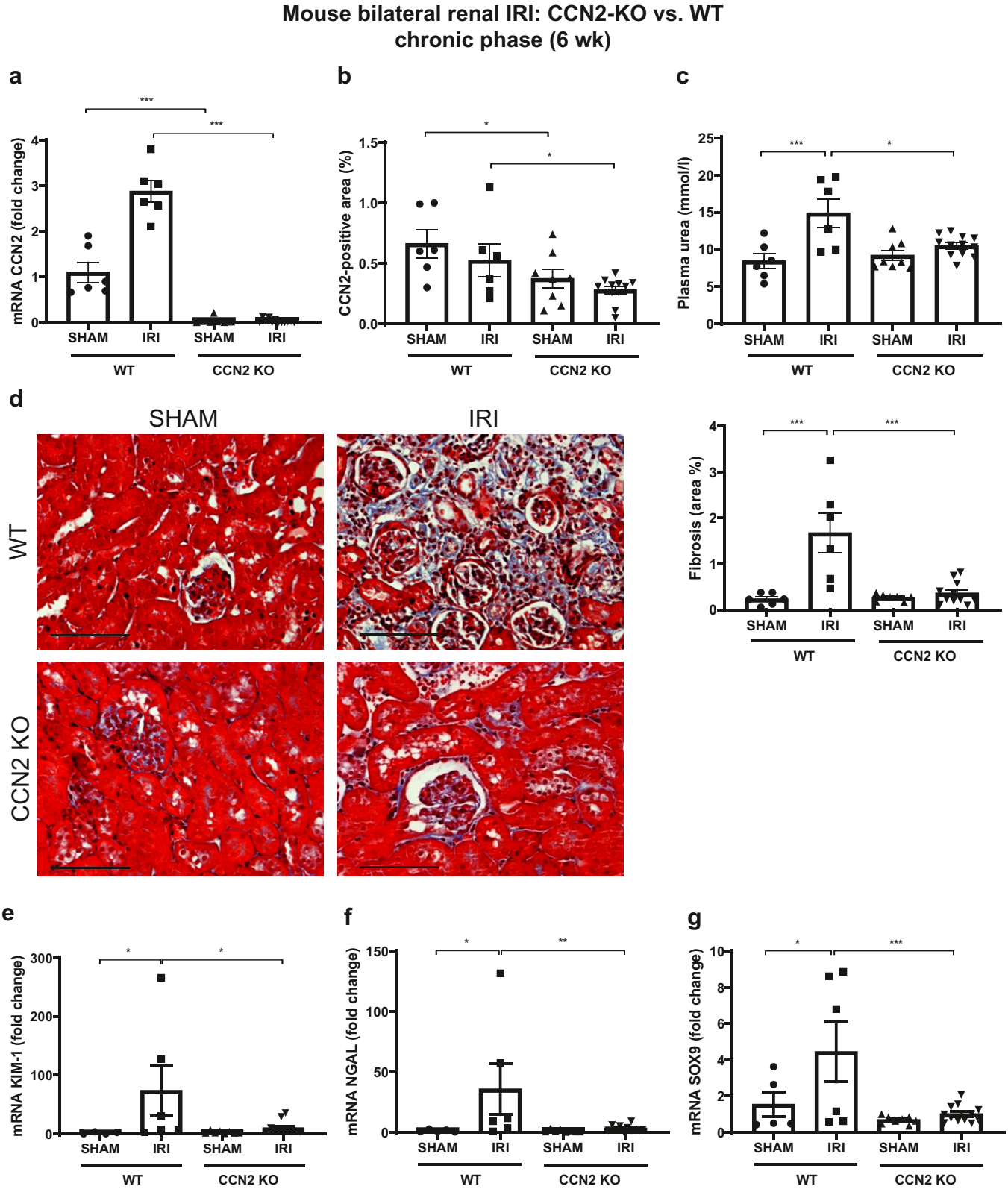

Figure 3 | Near total deletion of cellular communication network factor 2 (CCN2) expression reduces late tubulointerstitial fibrosis, functional decline, and persistent tubular injury 6 weeks after ischemia-reperfusion injury (IRI). (**a,b**) Quantitative real-time polymerase chain reaction (qPCR; **a**) and immunohistochemistry (**b**) analysis showed that CCN2 mRNA and protein expression were decreased after sham and IRI surgery in CCN2 knockout (KO) mice compared with wild-type (WT) mice. (**c**) Measurement of plasma urea levels showed that the decline in kidney function was reduced in CCN2 KO mice compared with WT mice. (**d**) Representative micrographs and quantification of mouse renal cortex stained with Masson's trichrome showed that increased tubulointerstitial fibrosis in IRI kidneys was decreased (continued)

cells treated with Lipofectamine vehicle. Cells were subjected to 24 hours of anoxia and 2 hours of reoxygenation.

The human kidney-2 (HK-2) human tubular epithelial cell line was cultured in Dulbecco's modified Eagle's medium supplemented with 5% fetal bovine serum. Semiconfluent HK-2 cells were infected with lentiviruses bearing a cytomegalovirus promoter-driven human CCN2 cDNA construct (LPP-L5140-Lv105) or control vector (GeneCopoeia) using 5 μg/ml polybrene in Dulbecco's modified Eagle's medium/5% fetal bovine serum for 24 hours. After a 24-hour recovery period, stable cultures were selected in 5 μg/ml puromycin containing media. To maintain selection pressure, media were changed every 3 days.

Plasma urea and creatinine

Plasma urea (DiaSys) and plasma creatinine (Arbor Assays) were measured using a colorimetric assay that conformed to the manufacturer's protocol.

Histology and immunohistochemistry

Tissue was fixed in a buffered 4% formalin solution for 24 hours and embedded in paraffin. Three-micrometer sections were mounted on adhesive slides (Leica Xtra), rehydrated through xylene and alcohol washes, and rinsed in distilled water. For periodic acid–Schiff and Masson's trichrome staining, standard procedures were used (Dako).

Immunohistochemistry for gamma H2AX (γH2AX) and CCN2 was performed as described previously, and immunohistochemistry for $p21^{CIP1}$ (p21) was set up based on the manufacturer's protocol.[28,29] First, endogenous peroxidase was blocked using H_2O_2, followed by antigen retrieval by boiling in pH6 citrate buffer and primary antibody incubation (*for human and mouse:* anti-γH2AX [pSer139], Novus Biologicals NB100-2280, 1:250; anti-CCN2, Santa Cruz sc-14939, 1:200; *for human*: anti-p21, Cell Signaling Technology #2947, 1:100; *for mouse:* anti-p21, Abcam ab188224, 1:4000; anti-Ki-67, Thermofisher RM9106S, 1:100; anti-cleaved caspase 3, BD Pharmingen 559565, 1:500) diluted in 1% bovine serum albumin blocking solution. For p21, CCN2, and Ki-67, secondary horseradish peroxidase–conjugated antibodies were applied and visualized using a Nova Red substrate (Vector Laboratories). For γH2AX and cleaved caspase 3, an alkaline phosphatase–conjugated antibody and liquid permanent red substrate (Dako) were used. Slides were counterstained with Mayer's hematoxylin.

Images were acquired using a Nikon Eclipse E800 microscope or scanned (Hamamatsu NanoZoomer) and digitally photographed in ImageScope to allow manual aligning of serial slides. For assessment of histopathologic damage, a kidney pathologist (TQN) blinded for experimental conditions graded acute tubular injury (ATI) on periodic acid–Schiff slides. ATI was graded on a scale from 0 to 3 as a percentage of the total cortical area of the tissue section (0 = 0%; 1 = <25%; 2 = <50%; 3 = >50%). ATI was defined as tubular dilatation, epithelial necrosis, cast formation, and loss of brush border.[30,31] For Masson's trichrome, positive area percentages were calculated based on 10 random microscopy images with original magnification ×200 using Photoshop CS6 (Adobe) and ImageJ1 (National Institutes of Health). For nuclear stains (γH2AX and p21), whole slides were scanned and the number of positive cells and total cells was calculated in QuPath.[32] For all scores, the score is displayed as the mean of the left and right kidney. In human biopsies, cortical tubules containing 1 or more positive cell(s) were annotated and manually counted using QuPath. For assessing the localization of positive staining, tubular structures were identified by kidney pathologists (TQN and RG). Tubular epithelial cells were defined as cross sections through tubular structures with basal membranes.

Quantitative real-time polymerase chain reaction

DNA and full RNA were extracted from kidney cortical poles using Trizol (Thermo-Fisher). Purity and quantity were determined using Nanodrop 2000 (Thermo-Fisher). For RNA analysis, a cDNA library was synthesized using 3 μg of RNA per kidney with SuperScript III reverse transcriptase (Thermo-Fisher). Quantitative real-time polymerase chain reactions were run on a ViiA 7 real-time polymerase chain reaction system (Applied Biosystems). The SYBR green primer sequences and Taqman probe quantitative real-time polymerase chain reaction are shown in Supplementary Table S1. To assess CCN2 DNA expression, we used intron/exon spanning SYBR green primers complementary to CCN2 intron2-exon3 and CCN2 exon4-intron4. For mRNA analysis, TATA-box binding protein was used as internal reference. Samples were run in duplicate. Samples free of mRNA and reverse transcriptase were used to control for potential contamination. The ΔΔCT method was used to calculate relative expression levels.

Western blot

RPTECs were lysed, and Western blot and ELISA analyses were performed as described previously.[27] Experiments were repeated 3 times. Membranes were incubated with antibodies for the following proteins: CCN2 (E2W5M; 1:1000; Cell Signaling Technology #10095), γH2AX (1:1000; Novus Biologicals NB110-2280), p21Waf1/Cip1 (1:1000, Cell Signaling Technology #37543), Ki-67 (1:1000, NBP2-22112, Novus Biologicals), GLB1 (1:1000, ab55176, Abcam), and β-actin (1:2500; Cell Signaling Technology #4967) for murine cultures and CCN2 (L-20 goat polyclonal; 1:1000; Santa Cruz-14939), p21 (1:1000; Cell Signaling-2947), plasminogen activator inhibitor-1 (PAI-1; 1:1000; #9163), and β-tubulin (1:1000; Abcam-ab6046) for human cultures. Furthermore, a mouse interleukin-6 ELISA Kit (Elabscience E-EL-M0044) was used.

Senescence-associated–β-galactosidase activity

Senescence-associated–β-galactosidase activity was performed following the manufacturer's protocol (Senescence Cells Histochemical Staining Kit, CS0030-1KT, 069M4101V, Sigma) after 72 hours of CCN2 stimulation.

Statistical analysis

Two-way analysis of variance with *post hoc* Tukey correction was used to compare the means of continuous variables in the 4 IRI groups. Discrete dependent variables in the IRI experiment and CCN2 administration experiments were tested nonparametrically with Mann-Whitney and Kruskal-Wallis with *post hoc* Dunn's test. Correlation of 2 independent variables was assessed using Pearson for continuous variables and Spearman for discrete variables. Values exceeding >1.5 interquartile ranges from the mean of a group were

Figure 3 | (continued) in CCN2 KO mice compared with WT mice. (**e–g**) qPCR analysis showed that increased mRNA expression of KIM-1 (**e**), NGAL (**f**), and SOX9 (**g**) in IRI kidneys was reduced in CCN2 KO mice compared with WT mice. Data are expressed as mean ± SEM (N = 4–6 for WT sham; N = 5–6 for WT IRI; N = 7–8 for KO sham; N = 11–13 for KO IRI). TATA-box binding protein was used as an internal control. *$P < 0.05$, **$P < 0.01$, and ***$P < 0.005$. Bar = 100 μm. To optimize viewing of this image, please see the online version of this article at www.kidney-international.org.

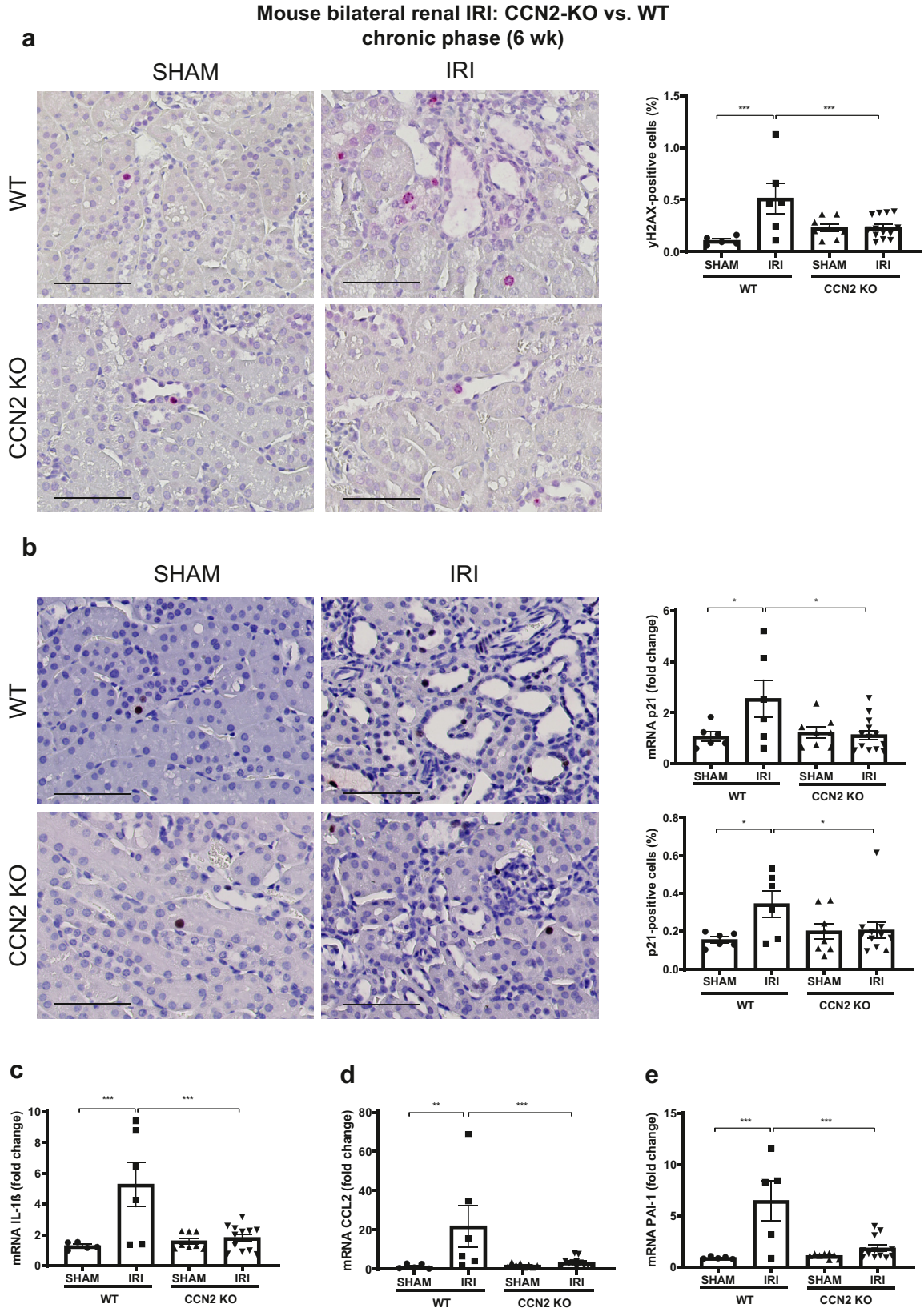

Figure 4 | Near total deletion of cellular communication network factor 2 (CCN2) expression reduces cellular senescence 6 weeks after ischemia-reperfusion injury (IRI). (**a,b**) Representative micrographs and quantification of mouse renal cortex stained with gamma H2AX (γH2AX; **a**) and p21CIP1 (p21; **b**) showed that increased DNA damage response in IRI kidneys was decreased in CCN2 knockout (KO) mice compared with wild-type (WT) mice. In addition, quantitative real-time polymerase chain reaction (qPCR) analysis showed (continued)

labeled as outliers and excluded. Data that showed abnormal distribution (i.e., right skewness) were log-transformed. Homogeneity of variances was tested with Levene's test because of unequal sample sizes. All statistical analyses were executed using the statistical program SPSS (IBM SPSS Statistics 25). Error bars represent SEM. P values < 0.05 were considered statistically significant.

RESULTS

Tubular CCN2 and DDR colocalize in acute IRI and subsequent tubulointerstitial fibrosis of the same kidney allograft

Phosphorylation of H2AX (γH2AX) marks DDR and induces CCA via the p53/p21 pathway.[33] P21 activation halts the cell cycle, usually transient in case of efficient DNA repair, but permanent in senescence.[34] Index case: histologic and immunohistochemical examination of a kidney allograft biopsy 8 months after transplantation revealed colocalization of tubular γH2AX, p21, and CCN2 in fibrotic areas (Figure 1a). Evaluation of a previous biopsy from that same allograft obtained for DGF 7 days after transplantation revealed colocalization of tubular γH2AX, p21, and CCN2 in areas with ATI (i.e., tubular dilatation, epithelial necrosis, cast formation, and loss of brush borders; Figure 1b).

Tubular CCN2 and DDR are associated with loss of kidney function in CAD biopsies

Tubular expression of γH2AX, p21, and CCN2 were assessed in kidney allograft biopsies taken for CAD (5–29 years after transplantation) or for DGF (6–8 days after transplantation) with no apparent cause other than tubulointerstitial fibrosis or IRI, respectively. Patient characteristics are shown in Supplementary Table S2. In CAD biopsies, estimated glomerular filtration rate correlated with γH2AX ($r = -0.73$; $P = 0.02$) and p21 ($r = -0.68$; $P = 0.04$) expression (Figure 2a and b). In addition, tendencies were observed between CCN2 and DDR in late biopsies (Supplementary Figure S1A and B), and in DGF biopsies between estimated glomerular filtration rate, DDR, and CCN2 (Supplementary Figure S1C–E) and CCN2 and DDR (Supplementary Figure S1F and G). Finally, *CCN2* mRNA colocalized with CCN2 protein, as well as γH2AX and p21 in CAD and DGF biopsies, indicating a tubular source of CCN2 transcription (Supplementary Figure S2).

CCN2 deletion reduces IRI-induced late tubulointerstitial fibrosis, functional decline, and persistent tubular injury

To study the association between CCN2 and kidney function, damage, fibrosis, and senescence, a 6-week IRI model was conducted using ROSA26Cre tamoxifen inducible CCN2 full KO mice. Tamoxifen-induced recombination resulted in a 99% reduction in CCN2 mRNA in both sham and IRI kidneys ($P < 0.005$; Figure 3a), as well as reduced CCN2 protein expression ($P = 0.03$ and $P = 0.04$, respectively; Figure 3b and Supplementary Figure S3). The plasma urea increase upon IRI was reduced by CCN2 KO ($P = 0.01$; Figure 3c). Similar trends for plasma creatinine were observed (Supplementary Figure S4A). Furthermore, tubulointerstitial fibrosis in Masson's trichrome staining was impeded by CCN2 KO ($P < 0.005$; Figure 3d). Concordantly, IRI-induced upregulation of gene expression levels of tubular injury markers *Kim-1* and *Ngal*, and of regeneration factor *Sox9* was reduced in CCN2 KO IRI mice ($P = 0.02$, $P = 0.009$, and $P < 0.005$; Figure 3e–g). Thus, CCN2-deficient mice had reduced tubular damage and fibrosis 6 weeks after IRI.

CCN2 deletion reduces IRI-induced late cellular senescence

To elucidate if senescence might be implicated in the fibrosis mitigating effect of CCN2 reduction, markers related to DDR, proliferation, p53 signaling, and SASP were analyzed by immunohistochemistry and quantitative real-time polymerase chain reaction. Reduced numbers of γH2AX-positive cells in CCN2 KO IRI mice indicated reduced DDR ($P < 0.005$; Figure 4a). The great majority of these cells were not cycling as evidenced by absent co-staining with Ki-67 (not shown). In addition, *p21* mRNA expression and the numbers of p21-positive cells in IRI kidneys were reduced by CCN2 KO ($P = 0.02$ and $P = 0.04$, respectively; Figure 4b). In CCN2 KO IRI kidneys, mRNA levels of SASP factors *Interleukin-1β*, *CC chemokine ligand 2*, and *Pai-1* were all reduced compared with WT IRI kidneys ($P < 0.005$, $P < 0.005$, and $P < 0.005$; Figure 4c–e). Of note, in WT IRI kidneys, γH2AX- and p21-positive cells were mainly PTECs in fibrotic areas of the outer cortex (Figure 4a and b). Overall, this indicated that CCN2-deficient mice had a reduced senescence phenotype 6 weeks after IRI.

CCN2 deletion preserves kidney function despite similar ATI marker expression at 3 days after IRI

To evaluate possible CCN2 involvement in early phases of the transition from acute IRI to the long-term profibrotic senescent state, a 3-day IRI model was performed. Tamoxifen administration resulted in a near total reduction of CCN2 mRNA in sham and IRI kidneys ($P < 0.005$; Figure 5a). The IRI-induced increases of plasma urea and creatinine were reduced in CCN2 KO mice ($P < 0.005$ and $P < 0.005$; Figure 5b and Supplementary Figure S4B, respectively). However, histologic examination of the cortices revealed similar degrees of acute tubular damage in WT and CCN2 KO IRI mice (Figure 5c). Concordantly, gene upregulation of

Figure 4 | (continued) that increased mRNA expression of p21 in IRI kidneys was reduced in CCN2 KO mice compared with WT mice. (**c–e**) qPCR analysis showed that increased mRNA expression of interleukin-1β (IL-1β) (**c**), CC chemokine ligand 2 (CCL2) (**d**), and plasminogen activator inhibitor-1 (PAI-1) (**e**) in IRI kidneys were reduced in CCN2 KO mice compared with WT mice. Data are expressed as mean ± SEM (N = 5–6 for WT sham; N = 5–6 for WT IRI; N = 8 for KO sham; N = 12–13 for KO IRI). TATA-box binding protein was used as an internal control. $^{*}P < 0.05$, $^{**}P < 0.01$, and $^{***}P < 0.005$. Bar = 50 μm. To optimize viewing of this image, please see the online version of this article at www.kidney-international.org.

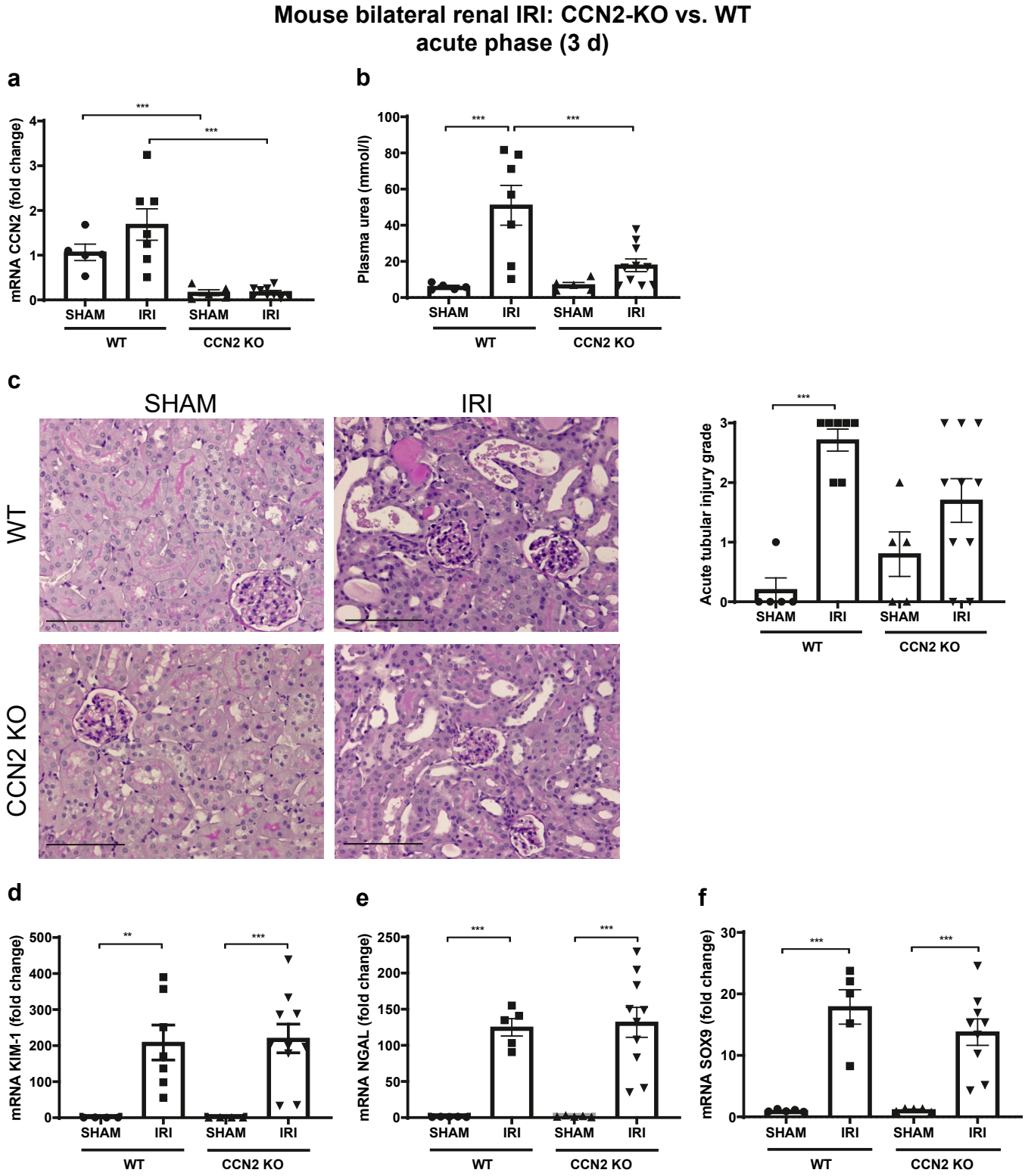

Figure 5 | Near total deletion of cellular communication network factor 2 (CCN2) expression preserves kidney function despite similar acute tubular injury 3 days after ischemia-reperfusion injury (IRI). (**a**) Quantitative real-time polymerase chain reaction (qPCR) analysis showed that CCN2 mRNA expression was decreased after sham and IRI surgery in CCN2 knockout (KO) mice compared with wild-type (WT) mice. (**b**) Measurement of plasma urea levels showed that the decline in kidney function was reduced in CCN2 KO mice compared with WT mice. (**c**) Representative micrographs and quantification of acute tubular injury histology of mouse renal cortex stained with periodic acid–Schiff (PAS) showed that increased acute tubular injury in IRI kidneys was not decreased in CCN2 KO mice compared with WT mice. (**d–f**) qPCR analysis showed increased mRNA expression of KIM-1 (**d**), NGAL (**e**), and SOX9 (**f**) in IRI kidneys in WT and CCN2 KO mice. Data are expressed as mean ± SEM (N = 4–5 for WT sham; N = 7 for WT IRI; N = 5 for KO sham; N = 10 for KO IRI). TATA-box binding protein was used as an internal control. $^{**}P < 0.01$ and $^{***}P < 0.005$. Bar = 100 μm. To optimize viewing of this image, please see the online version of this article at www.kidney-international.org.

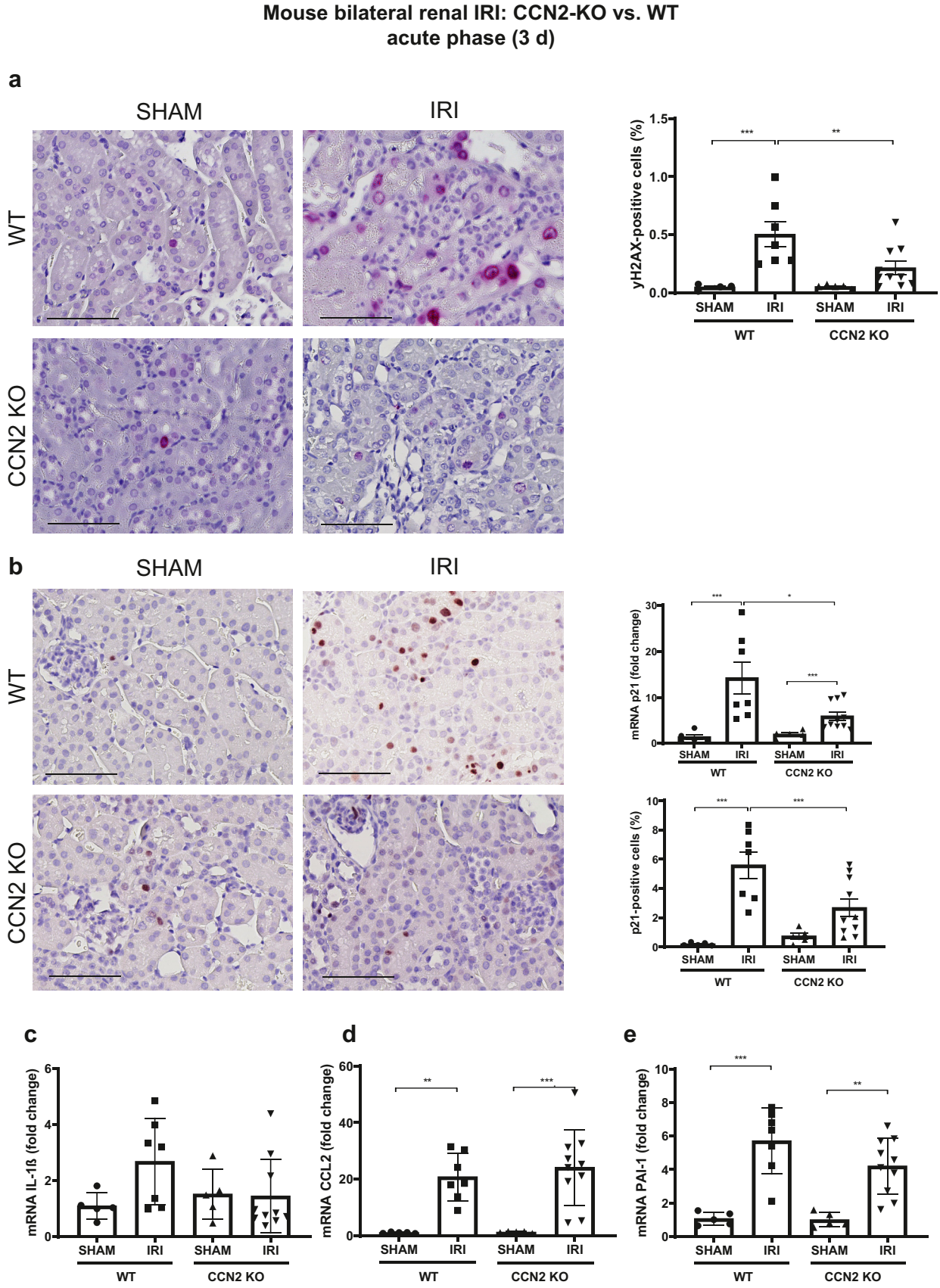

Figure 6 | Near total deletion of cellular communication network factor 2 (CCN2) expression reduces DNA damage and DNA damage response 3 days after ischemia-reperfusion injury (IRI). (**a**,**b**) Representative micrographs and quantification of mouse renal (continued)

tubular injury markers *Kim-1* and *Ngal* and regeneration factor SOX9 were equally upregulated in CCN2 KO as in WT kidneys (Figure 5d–f). In addition, IRI-induced proliferation and apoptosis of PTECs were similar in WT and CCN2 KO mice (Supplementary Figure S5).

CCN2 deletion reduces IRI-induced early DNA damage and DDR at 3 days after IRI

CCN2 KO IRI kidneys had lower numbers of γH2AX-positive cells ($P = 0.005$; Figure 6a) and lower p21 mRNA and protein expression ($P = 0.02$ and $P < 0.005$, respectively; Figure 6b), indicating reduced DNA damage and DDR. In WT IRI kidneys, γH2AX- and p21-positive cells were mainly PTECs localized in the inner cortex (Figure 6a and b). IRI-induced mRNA levels of SASP factors *Interleukin-1β*, *CC chemokine ligand 2*, and *Pai-1* were similar in KO and WT mice (Figure 6c–e). Furthermore, in CCN2 KO IRI mice, KO efficiency marked by CCN2 exon 3 DNA levels containing the floxed genomic site correlated with plasma urea, ATI grade, *Ngal* mRNA, *p21* mRNA, number of p21-positive cells, and *CC chemokine ligand 2* mRNA, and a trend was observed for *Ccn2* mRNA, *Kim-1* mRNA, *Sox9* mRNA, and *Pai-1* mRNA (Supplementary Figure S6). Overall, this indicated that CCN2-deficient kidneys had reduced DNA damage and DDR 3 days after IRI.

CCN2 induces DNA damage and DDR in PTECs

CCN2-induced DDR was evaluated in RPTECs and HK-2 cells. Stimulation of RPTECs with 100 ng/ml CCN2 increased the expression of γH2AX and p21 protein and had an antiproliferative effect marked by reduced Ki-67 expression ($P = 0.04$, $P = 0.02$, and $P = 0.08$, respectively; Figure 7a–d). Moreover, the mRNA expression of *p21* and SASP factors *Pai-1* and *CC chemokine ligand 2* ($P < 0.005$; Figure 7e–g), and senescence-associated–β-galactosidase activity ($P < 0.05$; Figure 7h) were increased by CCN2. In addition, in HK-2 cells, stable CCN2 overexpression resulted in increased expression of γH2AX, p21, and PAI-1 ($P = 0.001$, $P < 0.001$, and $P = 0.01$, respectively; Figure 7i–m) and an increased proportion of cells in the G2/M phase (Figure 7n).

CCN2 silencing reduces DNA damage and DDR induced by AR injury in PTECs

The direct impact of CCN2 on DDR in tubular cells was evaluated by silencing CCN2 in RPTECs subjected to AR injury, as an *in vitro* model for IRI.[35] AR injury–induced upregulation of CCN2, γH2AX, and p21 was alleviated when CCN2 was silenced, comparable with the expression levels of control cells that were cultured under normoxic conditions ($P = 0.007$; $P = 0.005$, and $P < 0.005$, respectively; Figure 8a–d). Conversely, increased Ki-67 expression suggested alleviation of CCA in CCN2-silenced AR-injured cells ($P < 0.005$; Figure 8a and e). Finally, the expression of GLB1, marking senescence-associated–β-galactosidase activity, was suppressed in CCN2-silenced cells ($P = 0.006$; Figure 8a and f).[36]

DISCUSSION

Our observations in human kidney allograft biopsies reveal an association of estimated glomerular filtration rate with tubular CCN2 expression, DDR, and cellular senescence, reflecting a sequence probably initiated by transplantation surgery–induced IRI. This is supported by our experimental data showing that CCN2 deletion preserves kidney function and reduces tubulointerstitial fibrosis and tubular senescence 6 weeks after IRI. Remarkably, this is preceded by preserved kidney function and reduced tubular DDR, despite similar acute tubular damage 3 days after IRI. The direct impact of CCN2 on proximal tubular DDR is further supported by *in vitro* data showing that CCN2 silencing in PTEC also reduces DDR and conversely, CCN2 administration induces p21 expression *in vivo* and *in vitro*. CCN2 has previously been shown to contribute to fibrosis development in CAD.[37,38] These novel findings suggest that CCN2 negatively contributes also to the acute response to IRI, in particular DNA damage and the DDR, thereby contributing to cellular senescence and fibrosis at later stages (Figure 9). This implicates that anti-CCN2 therapy may help to prevent post-IRI chronic kidney dysfunction by limiting IRI-induced acute DNA damage, senescent cell accumulation, and subsequent fibrosis.

These observations provide novel insights into the link between CCN2, senescence, and fibrosis on IRI. Several *in vitro* studies have suggested that CCN2 is a crucial factor in cellular senescence. For instance, CCN2 induces CCA in mesangial cells and bronchial epithelial cells, and a senescence phenotype in fibroblasts.[22,39–41] *In vivo*, CCN2 inhibition prevents fibrosis-induced CAD and PTEC-specific conditional CCN2 KO reduces IRI-induced fibrosis in combination with reduced G2/M arrest.[42,43] Accordingly, renal fibrosis elicited by folic acid was prevented in CCN2 KO mice.[44] Moreover, CCN2 induced G2/M arrest of tubular epithelial cells associated with the induction of fibrotic-related responses.[44] In human, anti-CCN2 therapy reduces

Figure 6 | (continued) cortex stained with gamma H2AX (γH2AX; **a**) and p21CIP1 (p21; **b**) showed that increased DNA damage response in IRI kidneys was decreased in CCN2 knockout (KO) mice compared with wild-type (WT) mice. In addition, quantitative real-time polymerase chain reaction (qPCR) analysis showed that increased mRNA expression of p21 in IRI kidneys was reduced in CCN2 KO mice compared with WT mice. (**c–e**) qPCR analysis showed that increased mRNA expression of interleukin-1β (IL-1β) (**c**), CC chemokine ligand 2 (CCL2) (**d**), and plasminogen activator inhibitor-1 (PAI-1) (**e**) in IRI kidneys were similar in CCN2 KO mice compared with WT mice. Data are expressed as mean ± SEM (N = 4–5 for WT sham; N = 6–7 for WT IRI; N = 4–5 for KO sham; N = 9–10 for KO IRI). TATA-box binding protein was used as an internal control. $^{*}P < 0.05$, $^{**}P < 0.01$, and $^{***}P < 0.005$. Bar = 50 μm. To optimize viewing of this image, please see the online version of this article at www.kidney-international.org.

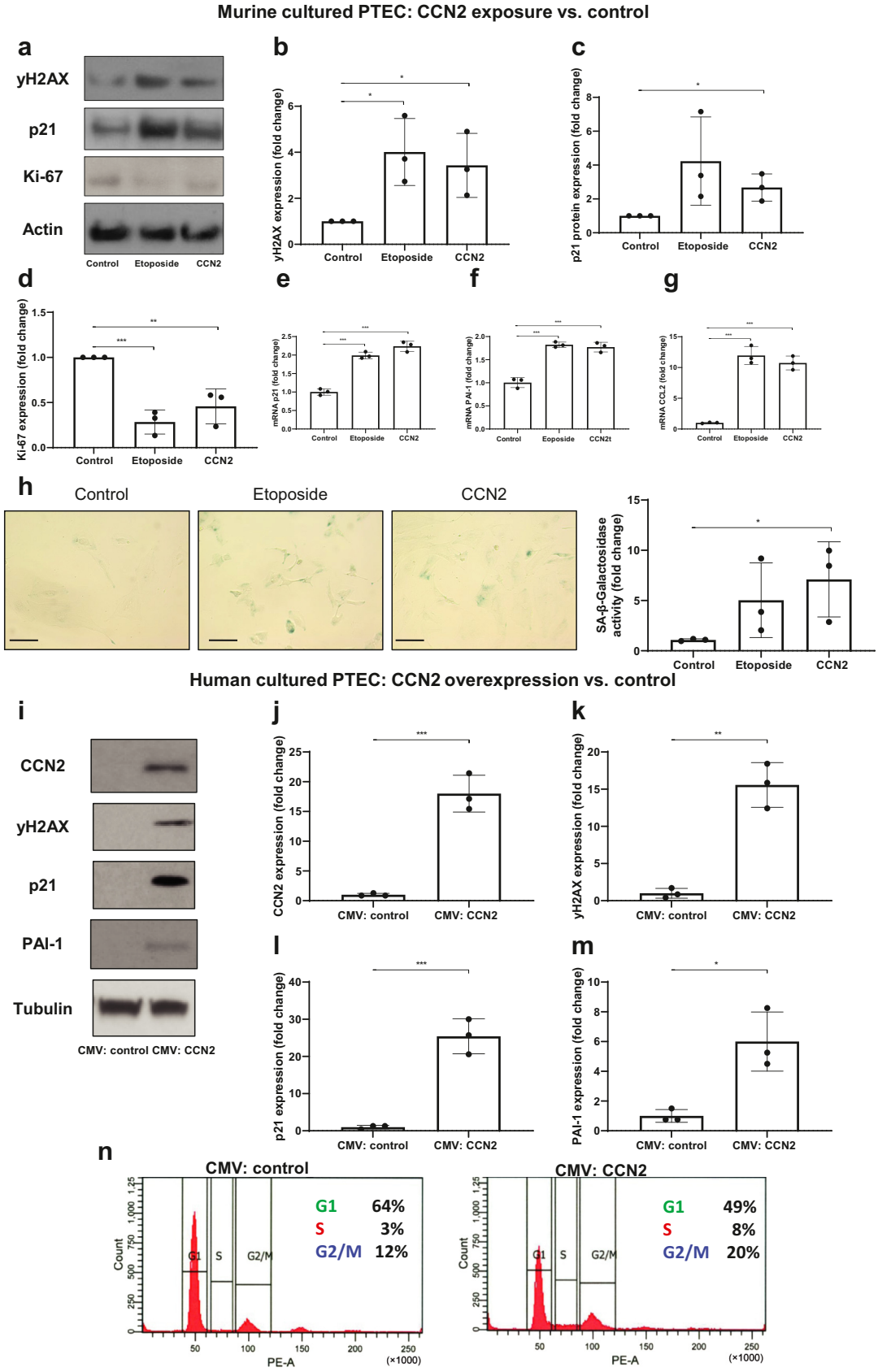

Figure 7 | Cellular communication network factor 2 (CCN2) induces DNA damage and DNA damage response (DDR) in cultured renal proximal tubular epithelial cells (PTECs). (**a**) Representative western blotting of protein extracts from cultured primary murine renal PTECs stimulated with 100 ng of CCN2 for gamma H2AX (γH2AX), p21CIP1 (p21), and Ki-67 showed that CCN2 increased DDR and (continued)

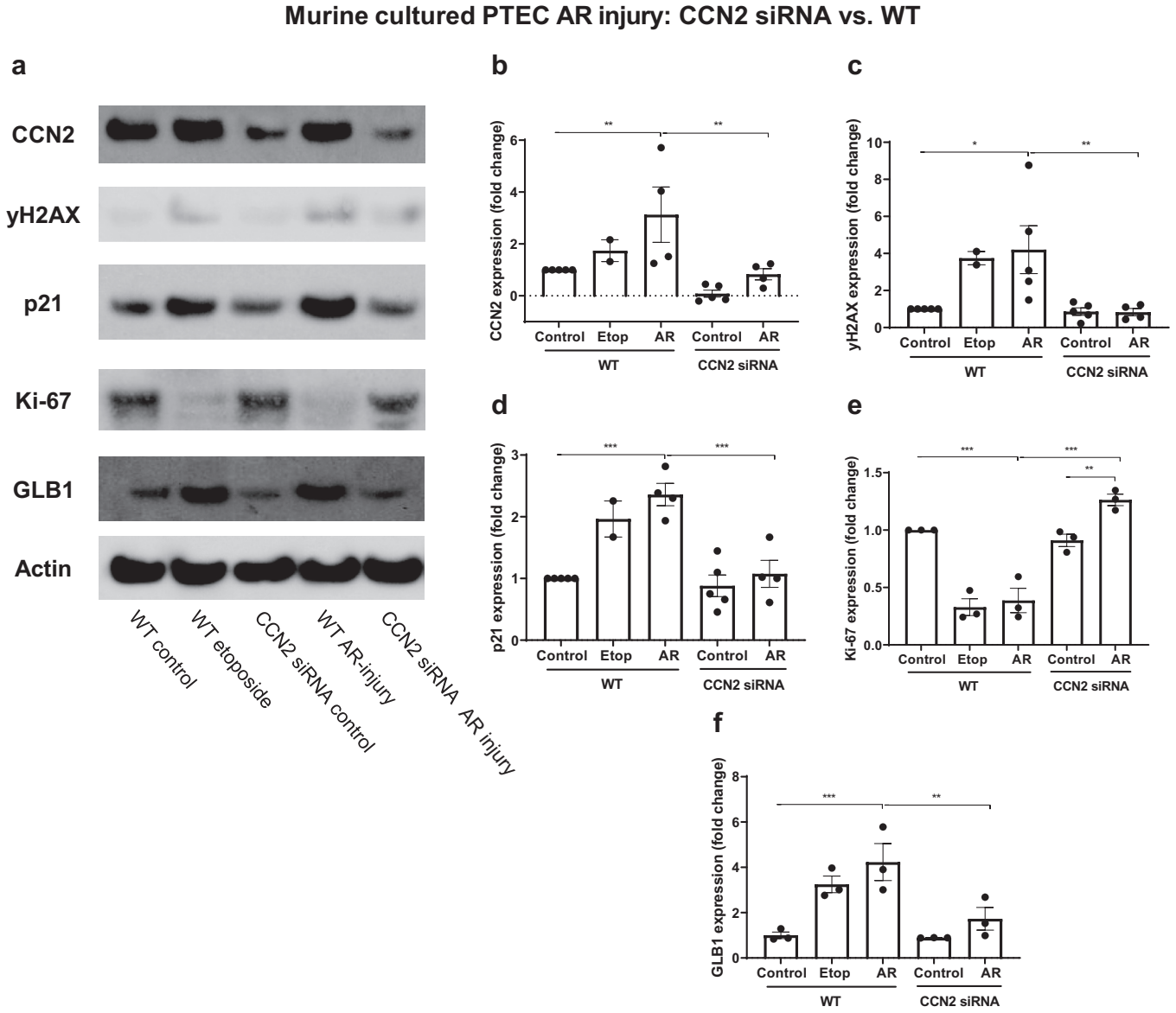

Figure 8 | Silencing of cellular communication network factor 2 (CCN2) alleviates DNA damage and DNA damage response (DDR) induced by anoxia-reoxygenation (AR) injury in cultured renal proximal tubular epithelial cells (PTECs). (**a**) Representative western blotting of protein extracts from cultured cells for CCN2, gamma H2AX (γH2AX), and p21CIP1 (p21) showed that increased DDR in AR-injured PTECs was alleviated by silencing of CCN2. Data represent 3 independent experiments. (**b–f**) Corresponding protein expression levels of CCN2 (**b**), γH2AX (**c**), p21 (**d**), Ki-67 (**e**), and GLB1 (**f**). Data are expressed as mean ± SEM relative to basal of 3 independent experiments. siRNA, small, interfering RNA; WT, wild type.

Figure 7 | (continued) reduced proliferation. (**b–d**) Corresponding protein expression levels of γH2AX (**b**), p21 (**c**), and Ki-67 (**d**). Data are expressed as mean ± SEM relative to basal of 3 independent experiments. (**e–g**) Quantitative real-time polymerase chain reaction analysis showed that CCN2 increased the mRNA expression of p21 (**e**), plasminogen activator inhibitor-1 (PAI-1) (**f**), and CC chemokine ligand 2 (CCL2) (**g**). Data are expressed as mean ± SEM. TATA-box binding protein was used as an internal control. (**h**) Representative micrographs and quantification of renal PTECs stained with senescence-associated (SA)–β-galactosidase stimulated with 100 ng of CCN2 showed that CCN2 induced senescence. Bar = 50 μm. (**i**) Representative western blotting of cell extracts isolated from human kidney-2 cells stably expressing empty vector (cytomegalovirus [CMV]-Control) and CCN2 construct (CMV-CCN2) at a similar confluence for CCN2, γH2AX, p21, and PAI-1 showed that CCN2 increased DDR and the expression of senescence-associated secretory phenotype factor PAI-1. (**j–m**) Corresponding protein expression levels of CCN2 (**j**), γH2AX (**k**), p21 (**l**), and PAI-1 (**m**). Data are expressed as mean ± SEM relative to basal of 3 independent experiments. (**n**) Flow cytometry analysis of propidium iodide–stained CMV-Control and CMV-CCN2 expressing cells determined the cell cycle distributions in the G1, S, G2/M phases as indicated. *$P < 0.05$, **$P < 0.01$, and ***$P < 0.005$. To optimize viewing of this image, please see the online version of this article at www.kidney-international.org.

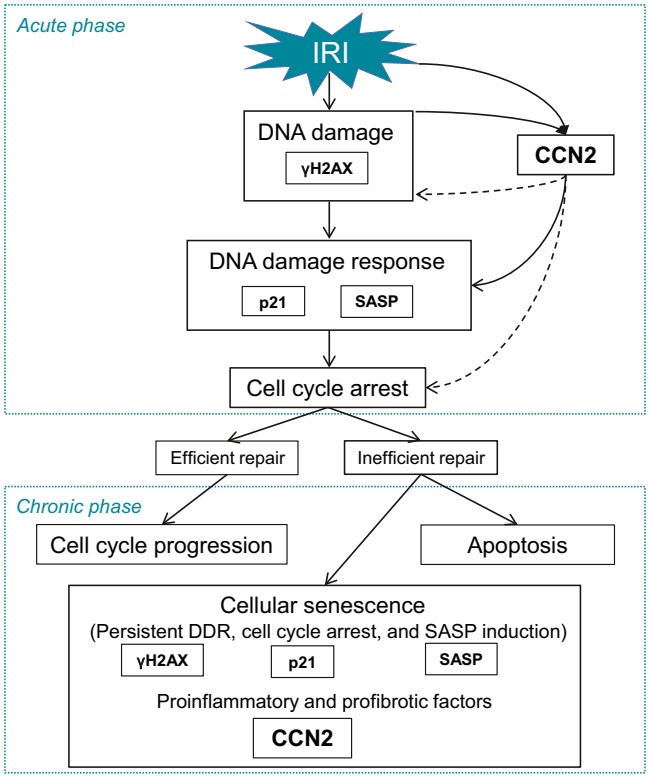

Figure 9 | Mechanisms involved in ischemia-reperfusion injury (IRI) linked with cellular communication network factor 2 (CCN2) in CCN2 knockout IRI mice. Near absence of CCN2 reduced the expression of gamma H2AX (γH2AX)- and p21CIP1 (p21)-positive cells, marking reduced DNA damage response and cell cycle arrest early after IRI. In the late phase upon IRI, this was followed by a sustained reduction in γH2AX- and p21-positive cells, along with reduced senescence-associated secretory phenotype (SASP), indicating reduced senescence phenotype. This coincided with reduced fibrosis and preserved kidney function. The dotted arrows are used to acknowledge that the exact mechanisms by which CCN2 contributes to senescent cell accumulation remain to be established.

albuminuria, an important predictor of chronic kidney disease, in diabetic patients with mild albuminuria.[45] However, the effects of CCN2 inhibition on senescence have not been investigated to date.

Beneficial effects of CCN2 expression on organ injury have also been observed. For instance, cardiac-specific CCN2 overexpression and postischemic administration of recombinant CCN2 protect the myocardium from acute IRI.[46] Also, CCN2 induces a SASP including antifibrotic matrix metalloproteinases in cultured fibroblasts and in specific stages of cutaneous wound healing, and reduces collagen formation in the latter.[22] This could be explained by a context-dependent beneficial antifibrotic role of cellular senescence in specific conditions, including cutaneous wound healing and on liver injury.[47,48] Negative effects of CCN2 inhibition have not been demonstrated in the setting of renal injury.

The main mechanisms of how CCN2 contributes to IRI-induced senescence might involve DDR and the SASP. IRI induces DNA damage in tubular epithelial cells and subsequent DDR to facilitate regeneration of the injured tubules.[49] Unresolved DNA damage leads to prolonged DDR, evolving in cellular senescence of the tubular epithelium within 3 days of injury that increases gradually over time.[50] CCN2-induced senescence in cultured cells is mediated through the accumulation of cell cycle regulators like p53 and p21.[22,39,40] Concordant with a role for CCN2 in the development of a senescence phenotype, we observed that DDR was attenuated in CCN2 KO mice in the early phase of IRI and in CCN2 inhibited PTEC subjected to AR injury, and conversely, that CCN2 induced p21 expression. This suggests that CCN2 affects the development of a senescence phenotype by altering DDR and subsequent CCA in the early phase upon renal injury.

The SASP promotes fibrosis and inflammation, reinforces the CCA, and contributes to paracrine senescence induction.[51–53] The development of the SASP relies on the activation of several transcription factors including nuclear factor κB.[51] CCN2 activates nuclear factor κB in murine kidneys, induces expression of SASP factors including interleukin-1β and matrix metalloproteinase-1 in cultured fibroblasts, and is itself also a constituent of SASP in senescent renal tubular epithelial cells.[19,20,22,51,54] Moreover, sustained tubular expression of the SASP factor PAI-1 promotes p21 expression, G2/M arrest, and fibrotic tubular maladaptive repair (including CCN2 upregulation).[55] In the late phase upon IRI, we observed that CCN2 KO mouse kidneys had reduced upregulation of SASP markers, suggesting that reduced autocrine and paracrine senescence induction might explain at least in part the association of reduced fibrosis with reduced accumulation of senescent cells.

In conclusion, our data add to the well-established role of CCN2 in kidney fibrosis providing evidence that it plays a role also early in the development of tubular damage and subsequent tubulointerstitial fibrosis after IRI, in particular in the DNA damage-DDR-cellular senescence-fibrosis sequence. This implies that CCN2-targeted therapy might benefit graft function and survival outcomes of patients who underwent kidney transplantation and warrants further evaluation of pharmacologic interventions in the early and later stages of transplant surgery–related IRI.

DISCLOSURE

FAV reported grants from University Medical Center Utrecht, during the conduct of the study. LLF reported grants from the Dutch Kidney Foundation, during the conduct of the study (Kolff Grant 17OKG20). RS reported grants from the Capital Region Medical Research Institute, during the conduct of the study. TQN and RG reported grants from the Dutch Kidney Foundation, during the conduct of the study (Consortium Grant CP1805 "TASKFORCE"). All other authors declared no competing interests.

ACKNOWLEDGMENTS

FAV is sponsored by and work was performed with a UMC Utrecht Alexandre Suerman stipend. LLF is sponsored by and work was performed with a Dutch Kidney Foundation Kolff-grant (17OKG20).

We are grateful for the generation of CCN2 condition knockout mice by Andrew Leask (Department of Physiology and Pharmacology, University of Western Ontario, London, Canada).

SUPPLEMENTARY MATERIAL

Supplementary File (PDF)

Supplementary Methods. RNA *in-situ* hybridization.

Figure S1. Tubular expression of cellular communication network factor 2 (CCN2) was not significantly associated with DNA damage response (DDR) in late kidney allograft biopsies nor with kidney function and DDR in early kidney allograft biopsies.

Figure S2. Tubular expression of cellular communication network factor 2 (CCN2) colocalized with DNA damage response (DDR) in late and early kidney allograft biopsies.

Figure S3. Near total deletion of cellular communication network factor 2 (CCN2) expression reduced CCN2 protein expression 6 weeks after ischemia-reperfusion injury (IRI).

Figure S4. Near total deletion of cellular communication network factor 2 (CCN2) expression results in reduced plasma creatinine 3 days after ischemia-reperfusion injury (IRI) and in similar plasma creatinine 6 weeks after IRI.

Figure S5. Near total deletion of cellular communication network factor 2 (CCN2) expression results in similar levels of proliferation and apoptosis 3 days after ischemia-reperfusion injury (IRI).

Figure S6. Cellular communication network factor 2 (CCN2) genetic knockout efficiency correlated with CCN2 mRNA, plasma urea, acute tubular injury, neutrophil gelatinase-associated lipocalin (NGAL) mRNA, p21 mRNA, and plasminogen activator inhibitor-1 (PAI-1) mRNA in CCN2 knockout (KO) mice 3 days after ischemia-reperfusion injury (IRI).

Table S1. Primers used for real-time polymerase chain reaction.

Table S2. Kidney transplant patient characteristics.

REFERENCES

1. Situmorang GR, Sheerin NS. Ischaemia reperfusion injury mechanisms of progression to chronic graft dysfunction. *Pediatr Nephrol*. 2019;34:951–963.
2. Li C, Yang CW. The pathogenesis and treatment of chronic allograft nephropathy. *Nat Rev Nephrol*. 2009;5:513–519.
3. Wekerle T, Segev D, Lechler R, Oberbauer R. Strategies for long-term preservation of kidney graft function. *Lancet*. 2017;389:2152–2162.
4. Lamb KE, Lodhi S, Meier-Kriesche H-U. Long-term renal allograft survival in the United States: a critical reappraisal. *Am J Transplant*. 2011;11:450–462.
5. Branzei D, Foiani M. Regulation of DNA repair throughout the cell cycle. *Nat Rev Mol Cell Biol*. 2008;9:297–308.
6. Gorgoulis V, Adams PD, Alimonti A, et al. Cellular senescence: defining a path forward. *Cell*. 2019;179:813–827.
7. Gire V, Dulic V. Senescence from G2 arrest, revisited. *Cell Cycle*. 2015;14:297–304.
8. de Keizer PLJ. The fountain of youth by targeting senescent cells? *Trends Mol Med*. 2017;23:6–17.
9. Wang WJ, Cai GY, XM C. Cellular senescence, senescence-associated secretory phenotype, and chronic kidney disease. *Oncotarget*. 2017;8:64520–64533.
10. Ferlicot S, Durrbach A, Bâ N, et al. The role of replicative senescence in chronic allograft nephropathy. *Hum Pathol*. 2003;34:924–928.
11. Melk A, Schmidt BM, Takeuchi O, et al. Expression of p16INK4a and other cell cycle regulator and senescence associated genes in aging human kidney. *Kidney Int*. 2004;65:510–520.
12. McGlynn LM, Stevenson K, Lamb K, et al. Cellular senescence in pretransplant renal biopsies predicts postoperative organ function. *Aging Cell*. 2009;8:45–51.
13. Günther J, Resch T, Hackl H, et al. Identification of the activating cytotoxicity receptor NKG2D as a senescence marker in zero-hour kidney biopsies is indicative for clinical outcome. *Kidney Int*. 2017;91:1447–1463.
14. Baker DJ, Childs BG, Durik M, et al. Naturally occurring p16 Ink4a-positive cells shorten healthy lifespan. *Nature*. 2016;530:184–189.
15. Baar MP, Brandt RMC, Putavet DA, et al. Targeted apoptosis of senescent cells restores tissue homeostasis in response to chemotoxicity and aging. *Cell*. 2017;169:132–147. e16.
16. Li C, Shen Y, Huang L, et al. Senolytic therapy ameliorates renal fibrosis postacute kidney injury by alleviating renal senescence. *FASEB J*. 2021;35:e21229.
17. Falke LL, Goldschmeding R, Nguyen TQ. A perspective on anti-CCN2 therapy for chronic kidney disease. *Nephrol Dial Transplant*. 2014;29(suppl 1):i30–i37.
18. Ramazani Y, Knops N, Elmonem MA, et al. Connective tissue growth factor (CTGF) from basics to clinics. *Matrix Biol*. 2018;68-69:44–66.
19. Sánchez-López E, Rayego S, Rodrigues-Díez R, et al. CTGF promotes inflammatory cell infiltration of the renal interstitium by activating NF-kappaB. *J Am Soc Nephrol*. 2009;20:1513–1526.
20. Yang L, Besschetnova TY, Brooks CR, et al. Epithelial cell cycle arrest in G2/M mediates kidney fibrosis after injury. *Nat Med*. 2010;16:143–535.
21. Wahab N, Cox D, Witherden A, Mason RM. Connective tissue growth factor (CTGF) promotes activated mesangial cell survival via up-regulation of mitogen-activated protein kinase phosphatase-1 (MKP-1). *Biochem J*. 2007;406:131–138.
22. Jun JI, Lau LF. CCN2 induces cellular senescence in fibroblasts. *J Cell Commun Signal*. 2017;11:15–23.
23. van Diest PJ. No consent should be needed for using leftover body material for scientific purposes. *BMJ*. 2002;325:648–651.
24. Kilkenny C, Browne WJ, Cuthill IC, et al. Improving bioscience research reporting: the ARRIVE guidelines for reporting animal research. *Osteoarthritis Cartilage*. 2012;20:256–260.
25. Fontes MS, Kessler EL, van Stuijvenberg L, et al. CTGF knockout does not affect cardiac hypertrophy and fibrosis formation upon chronic pressure overload. *J Mol Cell Cardiol*. 2015;88:82–90.
26. Kinashi H, Falke LL, Nguyen TQ, et al. Connective tissue growth factor regulates fibrosis-associated renal lymphangiogenesis. *Kidney Int*. 2017;92:850–863.
27. Eleftheriadis T, Pissas G, Golfinopoulos S, et al. Role of indoleamine 2,3-dioxygenase in ischemia-reperfusion injury of renal tubular epithelial cells. *Mol Med Rep*. 2021;23:472.
28. Lachaud C, Slean M, Marchesi F, et al. Karyomegalic interstitial nephritis and DNA damage-induced polyploidy in Fan1 nuclease-defective knock-in mice. *Genes Dev*. 2016;30:639–644.
29. Falke LL, Dendooven A, Leeuwis JW, et al. Hemizygous deletion of CTGF/CCN2 does not suffice to prevent fibrosis of the severely injured kidney. *Matrix Biol*. 2012;31:421–431.
30. Stokman G, Leemans JC, Claessen N, et al. Hematopoietic stem cell mobilization therapy accelerates recovery of renal function independent of stem cell contribution. *J Am Soc Nephrol*. 2005;16:1684–1692.
31. Pieters TT, Falke LL, Nguyen TQ, et al. Histological characteristics of Acute Tubular Injury during Delayed Graft Function predict renal function after renal transplantation. *Physiol Rep*. 2019;7:e14000.
32. Bankhead P, Loughrey MB, Fernández JA, et al. QuPath: open source software for digital pathology image analysis. *Sci Rep*. 2017;7:16878.
33. Fragkos M, Jurvansuu J, Beard P. H2ax is required for cell cycle arrest via the p53/p21 pathway. *Mol Cell Biol*. 2009;29:2828–2840.
34. Romanov VS, Pospelov VA, Pospelova TV. Cyclin-dependent kinase inhibitor p21(Waf1): contemporary view on its role in senescence and oncogenesis. *Biochemistry (Mosc)*. 2012;77:575–584.
35. Eleftheriadis T, Pissas G, Antoniadi G, et al. Cell death patterns due to warm ischemia or reperfusion in renal tubular epithelial cells originating from human, mouse, or the native hibernator hamster. *Biology (Basel)*. 2018;7:48.
36. Wagner J, Damaschke N, Yang B, et al. Overexpression of the novel senescence marker β-galactosidase (GLB1) in prostate cancer predicts reduced PSA recurrence. *PLoS One*. 2015;10:e0124366.
37. Vanhove T, Kinashi H, Nguyen TQ, et al. Tubulointerstitial expression and urinary excretion of connective tissue growth factor 3 months after renal transplantation predict interstitial fibrosis and tubular atrophy at 5 years in a retrospective cohort analysis. *Transpl Int*. 2017;30:695–705.
38. Vitalone MJ, O'Connell PJ, Wavamunno M, et al. Transcriptome changes of chronic tubulointerstitial damage in early kidney transplantation. *Transplantation*. 2010;89:537–547.
39. Abdel-Wahab N, Weston BS, Roberts T, Mason RM. Connective tissue growth factor and regulation of the mesangial cell cycle: role in cellular hypertrophy. *J Am Soc Nephrol*. 2002;13:2437–2445.

40. Jang JH, Chand HS, Bruse S, et al. Connective tissue growth factor promotes pulmonary epithelial cell senescence and is associated with COPD severity. *COPD*. 2017;14:228–237.
41. Capparelli C, Whitaker-Menezes D, Guido C, et al. CTGF drives autophagy, glycolysis and senescence in cancer-associated fibroblasts via HIF1 activation, metabolically promoting tumor growth. *Cell Cycle*. 2012;11: 2272–2284.
42. Luo GH, Lu YP, Song J, et al. Inhibition of connective tissue growth factor by small interfering RNA prevents renal fibrosis in rats undergoing chronic allograft nephropathy. *Transplant Proc*. 2008;40:2365–2369.
43. Inoue T, Kusano T, Amano H, et al. Cellular communication network factor 2 (CCN2) promotes the progression of acute kidney injury to chronic kidney disease. *Biochem Biophys Res Commun*. 2019;517: 96–102.
44. Rayego-Mateos S, Morgado-Pascual JL, Rodrigues-Diez RR, et al. Connective tissue growth factor induces renal fibrosis via epidermal growth factor receptor activation. *J Pathol*. 2018;244:227–241.
45. Adler SG, Schwartz S, Williams ME, et al. Phase 1 study of anti-CTGF monoclonal antibody in patients with diabetes and microalbuminuria. *Clin J Am Soc Nephrol*. 2010;5:1420–1428.
46. Ahmed MS, Gravning J, Martinov VN, et al. Mechanisms of novel cardioprotective functions of CCN2/CTGF in myocardial ischemia-reperfusion injury. *Am J Physiol Hear Circ Physiol*. 2011;300:H1291–H1302.
47. Krizhanovsky V, Yon M, Dickins RA, et al. Senescence of activated stellate cells limits liver fibrosis. *Cell*. 2008;134:657–667.
48. Demaria M, Ohtani N, Youssef SA, et al. An essential role for senescent cells in optimal wound healing through secretion of PDGF-AA. *Dev Cell*. 2014;31:722–733.
49. Zhou W, Otto EA, Cluckey A, et al. FAN1 mutations cause karyomegalic interstitial nephritis, linking chronic kidney failure to defective DNA damage repair. *Nat Genet*. 2012;44:910–915.
50. Jin H, Zhang Y, Ding Q, et al. Epithelial innate immunity mediates tubular cell senescence after kidney injury. *JCI Insight*. 2019;4:e125490.
51. Chien Y, Scuoppo C, Wang X, et al. Control of the senescence-associated secretory phenotype by NF-κB promotes senescence and enhances chemosensitivity. *Genes Dev*. 2011;25:2125–2136.
52. Myrianthopoulos V, Evangelou K, Vasileiou PVS, et al. Senescence and senotherapeutics: a new field in cancer therapy. *Pharmacol Ther*. 2019;193:31–49.
53. Xu M, Pirtskhalava T, Farr JN, et al. Senolytics improve physical function and increase lifespan in old age. *Nat Med*. 2018;24:1246–1256.
54. Liu L, Zhang P, Bai M, et al. p53 upregulated by HIF-1α promotes hypoxia-induced G2/M arrest and renal fibrosis in vitro and in vivo. *J Mol Cell Biol*. 2019;11:371–382.
55. Gifford CC, Lian F, Tang J, et al. PAI-1 induction during kidney injury promotes fibrotic epithelial dysfunction via deregulation of klotho, p53, and TGF-β1-receptor signaling. *FASEB J*. 2021;35:e21725.